Journal of Molecular Graphics and Modelling 38 (2012) 174–185

Contents lists available at SciVerse ScienceDirect

Journal of Molecular Graphics and Modelling

journal homepage: www.elsevier.com/locate/JMGM

# Structural significance of hypermodified nucleic acid base hydroxywybutine (OHyW) which occur at 37th position in the anticodon loop of yeast tRNA$^{Phe}$

Navanath M. Kumbhar[b], Bajarang V. Kumbhar[a], Kailas D. Sonawane[a,c,*]

[a] Structural Bioinformatics Unit, Department of Biochemistry, Shivaji University, Kolhapur 416004, Maharashtra (M.S.), India
[b] Department of Biotechnology, Shivaji University, Kolhapur 416004, Maharashtra (M.S.), India
[c] Department of Microbiology, Shivaji University, Kolhapur 416004, Maharashtra (M.S.), India

ARTICLE INFO

*Article history:*
Received 15 March 2012
Received in revised form 18 July 2012
Accepted 20 July 2012
Available online 26 July 2012

*Keywords:*
Transfer RNA
Hypermodified nucleoside
Hydroxywybutine
PM3
Molecular dynamics (MD) simulation

ABSTRACT

Conformational preferences of hypermodified nucleic acid base hydroxywybutine (OHyW) have been studied using quantum chemical single point semi-empirical PM3 method. Automated geometry optimization using semi-empirical RM1, molecular mechanics force field (MMFF) along with *ab-initio* HF-SCF (6-31G** basis set) and DFT (B3LYP/6-31G** basis set) calculations have also been made to compare the salient features. Molecular electrostatic potentials (MEPs) depict the polarities of hydroxywybutine (OHyW) side chain. Another conformational study showed that hydroxywybutosine side chain interacts with adjacent bases within the anticodon loop of tRNA$^{Phe}$. The solvent accessible surface area (SASA) calculations revealed the structural role of hydroxywybutine in anticodon loop. Explicit molecular dynamics (MD) simulation has been done over the PM3 most stable structure of OHyW. The hydroxywybutine side chain prefers 'distal' conformation i.e. spreads away from the cyclic five membered imidazole moiety of modified tricyclic guanine base. The predicted preferred conformation of hydroxywybutine may prevent extended Watson–Crick base pairing during protein biosynthesis process. This conformation of OHyW stabilized by intramolecular interactions between O(6)···HO(16), O(6)···HC(15) and O(20)···HC(17). Further stabilization is also expected from interactions between O(22)···HC(16) and O(23)···HC(15). Explicit molecular dynamics (MD) simulation over the PM3 most stable structure of OHyW support the preferred geometry by preserving the 'distal' orientation of hydroxywybutine side chain and intramolecular hydrogen bonding interactions. MD simulation study revealed the role of hydroxyl group of OHyW to avoid fluctuations and prevent multiple iso-energetic conformations of hydroxywybutine side chain as compared to wybutine (yW).



## 1. Introduction

At present nearly 100 modified nucleosides are found in tRNA. These modified nucleosides are produced by simple alkylation, hydrogenation, thiolation and isomerization of four common ribonucleosides such as adenosine (A), guanosine (G), cytosine (C) and uracil (U). Ribonucleosides are generally modified in the base and 2′-hydroxyl group of the ribose (sugar) by various tRNA modifying enzymes. However, some modifications involve complex chemical modifications which are characterized by the presence of the diverse functional group in the base substituent, such tRNA components are referred as hypermodified nucleosides [1,2]. Modifications occur more frequently at the first position (34th) and anticodon 3′-adjacent position (37th) of various tRNAs specific for diverse amino acids. Modified purine nucleosides such as wybutosine (yW), hydroxywybutosine (OHyW), N$^6$-threonylcarbamoyladenosine (t$^6$Ade) or 2-methylthio-N6-isopentenyladenosine (ms$^2$i$^6$A) and N6-hydroxynorvalylcarbamoyl adenine (hn$^6$Ade) are usually present at 37th position in tRNA [3]. The purine nucleosides (37th position) are always hypermodified when A or U present at 36th position in tRNA [3]. The wobble modifications are important for precise decoding mediated by codon–anticodon interactions [4], whereas modified nucleosides present at anticodon 3′-adjacent (37th) position maintains proper reading frame during protein biosynthesis process.

Hydroxywybutosine (OHyW) is a hydroxyl derivative of tricyclic hypermodified nucleoside wybutosine (yW) present at 3′-adjacent (37th) position in anticodon loop of tRNA$^{Phe}$ [5]. Transfer RNA$^{Phe}$ from rat liver also contains a hypermodified nucleoside Wye base (YOH) next to the 3′-end of the anticodon [5–7]. It has reported that tRNA$^{Phe}$ isolated from normal mouse neuroblastoma cells

* Corresponding author at: Structural Bioinformatics Unit, Department of Biochemistry, Shivaji University, Kolhapur 416004, Maharashtra (M.S.), India.
Tel.: +91 9881320719/231 2609153; fax: +91 231 2692333.
*E-mail address:* kds_biochem@unishivaji.ac.in (K.D. Sonawane).

1093-3263/$ – see front matter © 2012 Elsevier Inc. All rights reserved.
http://dx.doi.org/10.1016/j.jmgm.2012.07.005

has $m^1G$ instead of the naturally occurring modified nucleoside hydroxywybutosine (OHyW) while $tRNA^{Phe}$ from Ehrlich ascites tumor contains an undermodifed OHyW [8,9]. It has been found that methionine and lysine starvation on vero cells could block the formation of OHyW. This study was useful to investigate the proposed pathway of YOH biosynthesis [10,11]. On the basis of MS spectral data and negative coloring test for hydroxyl group, the fluorescent base isolated from rat liver $tRNA^{Phe}$ was identified as a β-hydroxywybutine [7]. Further, synthesis of β-hydroxywybutine of yeast $tRNA^{Phe}$ was also carried out by using dehydroxylation of the olifine followed by its cyclocondensation with $COCl_2$ and subsequent hydrogenolysis [12,13].

It has been reported that jumonji-related enzyme catalyzes the hydroxylation and peroxidation of wybutosine (yW) molecules to hydroxywybutosine (OHyW) and peroxywybutosine (o2yW), respectively [14]. The crystal structure of JmjC-domain-containing protein (hTYW5) in the free and complex forms with 2-OG and Ni(II) ion at 2.5 Å and 2.8 Å had shown that TYW5 enzyme synthesizes the OHyW in human by carbon hydroxylation using Fe(II) ion and Ni(II) ion as a cofactor [15]. It has been shown that the high hydrophobicity of purine nucleoside occur at anticodon 3′-adjacent position reinforces the codon–anticodon interactions by preventing incorrect Watson–Crick base pairing [16–18]. It was shown that the modified bases present at 37th position of tRNA anticodon loop could help stabilize the mRNA–tRNA pairing along with maintenance of reading frame [19,20].

Since the discovery of hydroxywybutosine in tRNA its structural role has not been studied at atomic level. Hence, in order to understand the structural and functional significance of chemical modification occur in guanine base at anticodon 3′-adjacent (37th) position of yeast $tRNA^{Phe}$, present conformational study of hypermodified nucleic acid base hydroxywybutine (OHyW) has been undertaken using quantum chemical methods and molecular dynamics (MD) simulation technique. It has found that the hydroxyl group of hydroxywybutine side chain would be useful to prevent multiple iso-energetic conformations as compared to wybutine base [21].

## 2. Nomenclature, conventions and approach

Fig. 1A illustrates the atom numbering and identification of the torsion angles which determine the relative orientation of various atoms in hypermodified nucleoside hydroxywybutine (OHyW). The torsion angle $\alpha$[C(12)-C(14)-C(15)-C(16)] was measured with respect to C(12) from the eclipsed (0°) position between the terminal bonds C(12)—C(14) and C(15)—C(16) in the right hand sense of rotation around the central bond C(14)—C(15). The other torsion angles $\beta$[C(14)—C(15)—C(16)—C(17)], $\gamma$[C(15)—C(16)—C(17)—N(18)], $\eta$[C(15)—C(16)—O(16)—H], $\delta$[C(16)—C(17)—C(22)—O(23)], $\psi 1$[C(17)—C(22)—O(23)—C(24)], $\psi 2$[C(22)—O(23)—C(24)—H], $\theta$[C(16)—C(17)—N(18)—C(19)], $\varphi 1$[C(17)—N(18)—C(19)—O(20)], $\varphi 2$[N(18)—C(19)—O(20)—C(21)] and $\omega$[C(19)—O(20)—C(21)—H] were measured cis (eclipsed, 0°) position in the right hand sense of rotation. For conformation with $\alpha = 180°$ the bond C(15)—C(16) point towards the five membered imidazole moiety of guanine base and the confirmation is termed 'proximal'. In case of $\alpha = 0°$ the bond C(15)—C(16) point away from the cyclic five membered purine ring and conformation is termed as 'distal'.

## 3. Computational methods

### 3.1. Conformational search of isolated hydroxywybutine

Conformational energy calculations have been performed with the help of quantum chemical single point semi-empirical PM3 method. All energy calculation steps and procedures performed by PM3 method are same as discussed in earlier conformational study of wybutine [21]. In conformational search polarities of the chemical bonds have been optimized for every molecular conformation. This method has been found widely useful in conformational studies of variety of organic and bioorganic molecules [22–24], including nucleic acid constituents [21]. Variation of total energy with respect to torsion angles determining the base substituent orientation in the modified hydroxywybutine (OHyW) has been investigated. One torsion angle changed at a time over the entire range of 0–360° at 30° intervals. Favored values of each torsion angle yielding energy minima are thus determined. By using these favored values various possible combinations for the set of dihedral angles are then tried out, and the combination yielding the overall minimum energy is selected. Starting with the conformation so arrived, each torsion angle was again individually varied over the entire range (0–360°) as already described. In this way, fine adjustments in the torsion angles lowering energy still further can be revealed. From these freshly arrived torsion angles new combinations of dihedral angles for stable molecular conformations may be derived as in the previous step. In this manner, the stability of the arrived conformation, with respect to changes in any of the various torsion angles, besides its preeminence was also ensured. In all PM3 calculations bond lengths and bond angles in the hydroxywybutine side chain have been retained from crystal structure data [25,26]. The PM3 method is implemented in commercially available PC Spartan Pro (version 6.1.1.0, Wavefunction Inc.) software [27]. Earlier conformational preferences of various modified nucleic acid bases and protonation induced conformational changes of these have been studied [28–34].

### 3.2. Molecular electrostatic potentials (MEPs) and solvent accessible surface calculations (SASA)

The molecular electrostatic potentials are calculated on the optimized geometry of the hydroxywybutine (OHyW) using PC Spartan Pro (version 6.1.1.0, Wavefunction Inc.) software [27]. Entire accessible surface of the OHyW molecule considered for the calculation of MEPs. The color coded surface gives information of size of molecular surface and the location of positive and negative electrostatic potentials. The positive electrostatic potentials indicated by the deepest blue color that is repulsion of positive charges whereas negative electrostatic potentials showed by deepest red color indicating the attraction of positive charges. The solvent accessible surface area (SASA) of anticodon loop structure of $tRNA^{Phe}$ has been calculated using Chimera [35].

### 3.3. Conformation of hydroxywybutosine in tRNA anticodon loop using PCILO method

Conformational behavior of hydroxywybutosine in context of other anticodon loop bases has also been performed in gaseous state using quantum chemical Perturbative Configuration Interaction using Localized Orbital (PCILO) method. PCILO method has been found useful in conformational studies of bio-organic molecules [36,37], as well as for various hypermodified nucleosides [28,34]. The ribose-phosphate backbone has been adopted from yeast $tRNA^{Phe}$ crystal structure [26]. The conformational search of hydroxywybutosine side chain in $tRNA^{Phe}$ anticodon loop has been performed similarly as explained for isolated hydroxywybutine in Section 3.1 of this manuscript.

### 3.4. Automated geometry optimization

Relative stability of salient points has been examined using automated complete geometry optimization calculations through

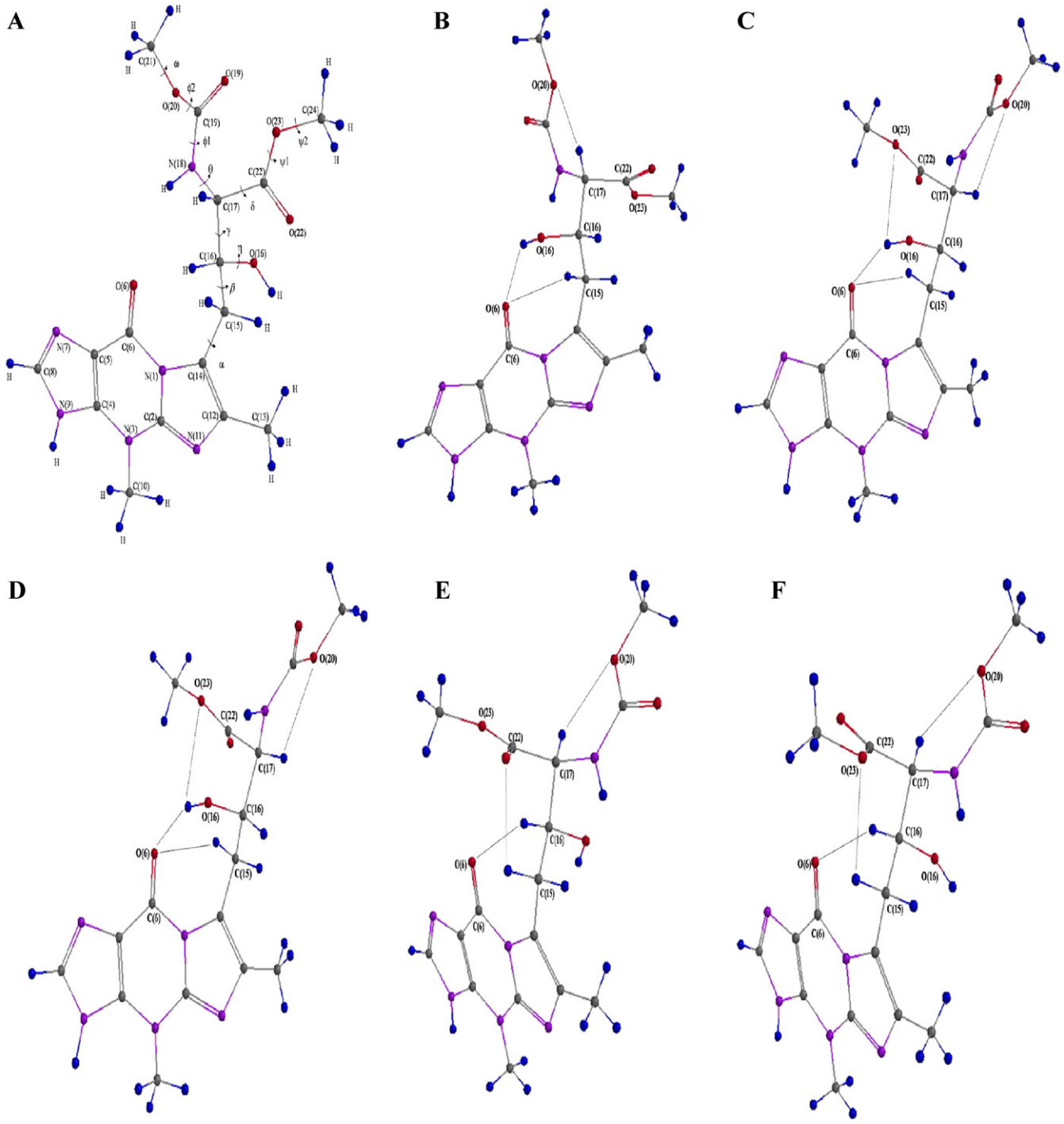


**Fig. 1.** Shows (A) nomenclature and convention system for hydroxywybutine (OHyW) side chain torsion angles, (B) PM3 most stable structure of OHyW, (C) first higher energy (1.73 kcal/mol) alternative stable conformation of OHyW, (D) second higher energy (2.15 kcal/mol) alternative stable conformation of OHyW. (E) Third higher energy (3.1 kcal/mol) alternative stable conformation of OHyW and (F) fourth higher energy (3.7 kcal/mol) alternative stable conformation of OHyW.

semi-empirical RM1 and molecular mechanics force field (MMFF) methods [38,39]. The preferred conformation of isolated hydroxywybutine (OHyW) has also been tested at *ab-initio* level using molecular orbital Hartree–Fock (HF-SCF) quantum mechanical energy calculations (6-31G** basis set) and density functional theory (DFT) (B3LYP/6-31G** basis set) [40,41].

The most stable conformation of hydroxywybutosine which occur at 37th position in anticodon loop of $tRNA^{Phe}$ has also been optimized using MMFF and RM1 methods. These methods (RM1, MMFF, HF-SCF and DFT) are implemented in commercially available *PC Spartan Pro* (version 6.1.1.0, Wavefunction Inc.) software [27].

### 3.5. Molecular dynamics (MD) simulation protocol

Molecular dynamics (MD) simulations were performed using Sybyl 7.3 (TRIPOS Associates, 2006) commercial software from Tripos, Inc. in order to highlight the influence of water on

**Table 1**
Shows hydrogen bonding interactions from PM3 preferred conformation of hydroxywybutine (OHyW) and its alternative structures.

| Atoms involved (1-2-3) | Distance atom pair 1-2 (Å) | Distance atom pair 2-3 (Å) | Angle 1-2-3 (°) | Fig. ref. |
|---|---|---|---|---|
| O(6)···HC(15) | 2.428 | 1.073 | 110.91 | 1B and C |
| O(6)···HO(16) | 1.956 | 0.958 | 152.62 | 1B and C |
| O(20)···HC(17) | 2.583 | 1.070 | 94.61 | 1B–E |
| O(6)···HC(16) | 1.960 | 1.073 | 135.30 | 1E and F |
| O(23)···HO(16) | 2.604 | 0.958 | 90.00 | 1C |
| O(22)···HC(15) | 2.504 | 1.073 | 110.20 | 1C–E |
| O(23)···HC(16) | 2.795 | 1.073 | 96.21 | 1D and E |
| O(22)···HC(16) | 2.754 | 1.073 | 96.00 | 1B and F |
| O(23)···HC(15) | 2.524 | 1.073 | 111.41 | 1B and F |

hydroxywybutine side chain. Similarly, such MD simulations were also performed to see the influence of solvation on the peptide nucleic acid [42]. The PM3 predicted preferred conformation of hydroxywybutine (Fig. 1B) was used as a starting geometry for molecular dynamics simulation study. The calculations were performed on HP xw8600 workstation. Molecular dynamics simulation protocol similar to earlier study has been employed [21,34]. Kollman-all-atom force field [43] with Gasteiger–Marsilli charges and TIP3P model water has been chosen for MD simulation study. Minimal cubic periodic boundary condition of diameter 31.519 Å has been applied. Trajectories are taken for time span of 10 ps. The constant temperature (canonical ensemble) simulation at 300 K has been used along with 8 Å non bonded cut off and dielectric function 'constant' held at 1. For temperature ramp from 0 K to 200 K, 10 ps interval of 50 K and for 200–300 K, 10 ps interval of 25 K temperature steps were used. The other usual conditions applied include 1 fs time step, initial Boltzmann velocity distribution, and shake algorithm for hydrogen atoms, 10 fs non-bonded update with scaled velocities. To remove steric clashes initially, 5000 cycles of steepest descent minimization steps are applied to the whole system. This minimized system considered for 200 ps equilibration protocol followed by 5000 cycles of steepest descent energy minimization. Final system is subjected for 5 ns of production run time by maintaining all the parameters as described earlier.

## 4. Results and discussion

### 4.1. Conformational preferences of hydroxywybutine (OHyW) using semi-empirical PM3 method

Fig. 1B depicts the PM3 predicted preferred conformation of isolated hydroxywybutine (OHyW) describing torsion angle values as mentioned in Table 2. Preferred orientation of hydroxywybutine side chain is such that methoxycarbonyl-aminocarboxypropyl group spreads away 'distal' from the five membered imidazole moiety of modified tricyclic guanine base. Such kind of 'distal' orientation has also been observed for wybutine molecule [21]. The carbonyl O(6) of modified tricyclic base involved in hydrogen bonding with HO(16) and HC(15) of hydroxywybutine side chain (Table 1). In addition with these basic interactions, hydrogen bonding between O(20).HC(17) help maintain 'distal' orientation of OHyW side chain. Preferred conformation of OHyW is stabilized by intramolecular hydrogen bonding interactions between O(6)···HO(16), O(6)···HC(15) and O(20)···HC(17). Additional stabilization is also expected from interactions between O(23)···HC(15) and O(22)···HC(16). Such C═O···HC interactions have also been found important in the conformational study of wybutine [21] as well as in case of other molecules [49–56]. The bifurcated hydrogen bonding interactions between HO(16)···O(6)···HC(15) (Fig. 1B) could be useful to maintain 'distal' conformation of hydroxywybutine similar to NH(18)···O(6)···HC(15) and NH(18)···O(6)···HC(16) found in case of wybutine [21]. Such bifurcated interactions are also found useful to provide structural stability as discussed in some other studies [31,57–60].

Extended nature of $\beta$ torsion angle along with eclipsed orientation taken by $\eta$ torsion angle favors the existence of hydrogen bonding between O(6)···HO(16). This interaction specifies $\alpha = 270^\circ$ torsion angle value, which is deviated by approximately 180° from wybutine preferred conformation and crystal structure value. The atom HO(16) of hydroxywybutine (OHyW) could restrict fluctuations around torsion angles $\alpha$, $\beta$, $\gamma$ and $\delta$ in order to avoid multiple iso-energetic conformations as observed in case of wybutine (yW) side chain [21]. The carboxy methyl (—$COOCH_3$) group of hydroxywybutine side chain i.e. C(22)—O(22)—O(23)—$CH_3$ orient towards the —$CH_3$ group of five membered tricyclic ring. This kind of orientation could be possible because of the rotation of torsion angles $\gamma = 60^\circ$, $\eta = 330^\circ$ and $\delta = 90^\circ$ which would allow interactions between O(22)···HC(16) and O(23)···HC(15). This orientation of carboxy methyl (—$COOCH_3$) group of hydroxywybutine (OHyW) side chain could allow certain kind of interactions with codons if present at 3′-end and such interactions are also discussed in the earlier studies [44,45].

Besides PM3 predicted preferred conformation, conformational energy calculations have also been carried out to search the higher energy alternative stable conformations (Table 2) of hydroxywybutine (OHyW). These alternative conformations show different torsion angles and hydrogen bonding interactions (Tables 1 and 2). Fig. 1C depicts the first higher energy (1.73 kcal/mol) alternative stable conformation of OHyW arises due to flipping of $\gamma$ torsion angle by 120° from its preferred value (Fig. 1B and Table 2) and positioned to 180°. This change in $\gamma$ torsion angle could lead to replace the hydrogen bonding interaction between O(23)···HC(15) by O(22)···HC(15). In addition to this a new interaction between O(23)···HO(16) could be an additional stabilizing factor. Second higher energy (2.15 kcal/mol) alternative stable conformation (Fig. 1D) resulted by flipping of $\alpha$ and $\delta$ torsion angles by 210° and 180°, respectively, from their respective preferred values (Table 2) and positioned to $\alpha = 120^\circ$ and $\delta = 270^\circ$. This alternative conformation replace the hydrogen bonding interactions between O(6)···HC(15) by O(6)···HC(16), O(23)···HC(15) by O(22)···HC(15) and O(22)···HC(16) by O(23)···HC(16). Next higher energy (3.1 kcal/mol) alternative stable conformation (Fig. 1E) arises by flipping of $\alpha$ by 210°, $\eta$ by 120° and $\delta$ by 180° from

**Table 2**
PM3 predicted higher energy alternative stable conformations of hydroxywybutine (OHyW).

| Torsion angles (°) | Rel. energy kcal/mol | Fig. ref. |
|---|---|---|
| $\alpha = 270^\circ$, $\beta = 180^\circ$, $\gamma = 60^\circ$, $\eta = 330^\circ$, $\delta = 90^\circ$, $\psi 1 = 180^\circ$, $\psi 2 = 180^\circ$, $\theta = 150^\circ$, $\varphi 1 = 0^\circ$, $\varphi 2 = 180^\circ$, $\omega = 180^\circ$ | 0.0 | 1B |
| $\gamma = 180^\circ$ | 1.73 | 1C |
| $\alpha = 120^\circ$, $\delta = 270^\circ$ | 2.15 | 1D |
| $\alpha = 120^\circ$, $\eta = 90^\circ$, $\delta = 270^\circ$ | 3.10 | 1E |
| $\alpha = 120^\circ$ | 3.70 | 1F |

their respective preferred values (Fig. 1B). This alternative structure preserved all salient features observed in the second alternative conformation (Fig. 1D). Further higher energy (3.7 kcal/mol) alternative stable structure (Fig. 1F) may be possible due to flipping of $\alpha$ torsion angle by 210° from its preferred value and positioned to $\alpha$ = 120°, which resulted in substitution of interaction between O(6)···HC(15) by O(6)···HC(16) (Fig. 1B). The bifurcated interactions between O(23)···HO(16)···O(6) and HO(16)···O(6)···HC(15) observed in PM3 alternative stable structures (Fig. 1B–D) support the 'distal' conformation of OHyW. These kinds of bifurcated interactions have been discussed in some other studies [31,57–60].

### 4.2. Full geometry optimization of hydroxywybutine (OHyW)

In order to compare the salient features from the preferred conformation of hydroxywybutine (Fig. 1B), automated complete geometry optimization has also been made using quantum chemical RM1 and molecular mechanics force field (MMFF) methods. The most stable structure obtained by PM3 method has been tested at *ab-initio* level using HF-SCF (6-31G** basis set) and DFT (B3LYP/6-31G** basis set) methods and results are shown in Table 3. RM1 optimization significantly preserves initial geometry (Fig. 1B and Table 2). Torsion angles $\eta$ and $\delta$ are deviated by 29–35° from the preferred values (Fig. 1B) while other torsion angles $\alpha$, $\beta$, $\gamma$, $\psi$1, $\psi$2, $\theta$, $\varphi$1, $\varphi$2 and $\omega$ have minor differences of 10–15°. Optimized conformation retain hydrogen bonding interactions between O(6)···HC(15), O(6)···HO(16), O(20)···HC(17) and O(22)···HC(16), which are similar to the preferred conformation (Table 1). MMFF optimization over the PM3 preferred structure (Fig. 1B and Table 3) shows that the torsion angles $\delta$, $\eta$ and $\varphi$1 differs by 10–35° whereas other torsion angles show negligible variations. Optimization performed through *ab-initio* HF-SCF (6-31G** basis set) calculation also preserved initial geometry. Minor difference of 10–30° found in $\beta$, $\eta$ and $\delta$ torsion angles while remaining torsion angles show negligible (0–10°) change as compared to preferred conformation (Fig. 1B and Table 2). Optimized structure retain interactions between O(6)···HC(15), O(6)···HO(16) and O(22)···HC(16) as compared to the preferred conformation (Fig. 1B). Full geometry optimization performed by DFT (B3LYP/6-31G** basis set) method resulted in maintaining the preferred geometry with hydrogen bonding interactions as found in the most stable structure (Fig. 1B). Hence, all these optimized results (Table 3) support the PM3 most stable conformation (Fig. 1B) of hydroxywybutine by preserving preferred hydrogen bonding interactions and initial geometry.

### 4.3. Molecular dynamics (MD) simulation study over PM3 most stable conformation

Explicit molecular dynamics simulation up to 5 ns has been performed over the PM3 most stable conformation (Fig. 1B) to check the conformational flexibility and hydration effect on the hydroxywybutine (OHyW) side chain. The MD simulation results are shown in Figs. 2–4, whereas geometrical parameters of average and snapshot structures are depicted in Table 4. For analysis purpose we selected four average structures particularly at 0–1000 ps (Fig. 2A), 1310–1470 ps, 2000–2200 ps (Fig. 2B) and 4900–5000 ps (Fig. 2F) and three snapshot structures particularly at 2650 ps (Fig. 2C), 3590 ps (Fig. 2D) and 4410 ps (Fig. 2E). The average structure obtained at 0–1000 ps (Fig. 2A) show minor variation in the side chain torsion angles of hydroxywybutine (OHyW) as shown in Table 2. This average structure maintained intramolecular hydrogen bonding between O(6)···HO(16), O(6)···$H_1$C(15) and O(23)···$H_2$C(15) as like PM3 preferred structure of hydroxywybutine (Fig. 1B). The hydroxywybutine side chain preserves distal conformation throughout the 5 ns simulation period. Next average structure (Table 4) chosen for the period 1310–1470 ps when $\alpha$ torsion angle flipped by 210° as compared to preferred structure of OHyW (Fig. 1B). This average structure show similar torsion angle values and interactions such as O(6)···HC(15) and O(6)···HC(16) as found in earlier conformational study of wybutine [21] and crystal conformer 1EHZ.pdb [25]. This average structure shows close resemblance with 2nd, 3rd and 4th alternative stable structures of OHyW (Fig. 1D–F) in terms of torsion angle values and hydrogen bonding interactions. Average structure taken at 2000–2200 ps (Fig. 2B) retain similar torsion angle values as compared to the most stable (Fig. 1B) and alternative stable structures (Fig. 1D–F). The average structure (Fig. 2B) also maintain hydrogen bonding interactions (Table 2) such as O(6)···$H_2$C(15), O(6)···HC(16) and O(20)···HC(17). In this average structure HO(16) interacts with O(23) instead of O(6) of tricyclic base, this interaction might be helpful to minimize fluctuations occurred in the $\delta$ torsion angle (Table 2). Average structure (Fig. 2F) selected at last 100 ps i.e. 4900–5000 ps also preserve interactions O(6)···$H_2$C(15), O(6)···HC(16) and O(23)···$H_2$C(15) as found in the PM3 preferred (Fig. 1B) and alternative stable conformations (Fig. 1C–F) of OHyW and shown in Table 4. Another average structure (Fig. 2B) maintain distal conformation for hydroxywybutine side chain as like PM3 most stable structure of OHyW (Fig. 1B).

Snapshot structure taken at 2650 ps (Fig. 2C) was analyzed and results are depicted in Table 4. This snapshot structure retains basic hydrogen bonding interactions as observed in PM3 most stable structure (Fig. 1B) as well as crystal structure [25]. The atom HO(16) interacts with O(22) instead of O(6) of tricyclic base in order to maintain distal conformation of hydroxywybutine side chain. Second snapshot structure taken at 3590 ps (Fig. 2D) also preserve basic hydrogen bonding interactions such as O(6)···$H_2$C(15), O(6)···HC(16) and O(20)···HC(17) similar to PM3 most stable and its alternative stable conformations (Table 1). Snapshot structure taken at 4410 ps (Fig. 2E) depict small differences in the side chain torsion angles but preserve hydrogen bonding interactions between O(6)···$H_2$C(15), O(6)···HC(16) and O(20)···HC(17) as compared to PM3 most stable conformation (Fig. 1B and Table 1). Hydrogen bonding interactions between O(6)···$H_2$C(15) and O(20)···HC(17) observed in PM3 most stable structure (Fig. 1B) and crystal structure [25] are also well maintained during 5 ns MD simulation. The average (Fig. 2A, B and F) and snapshot (Fig. 2C–E) structures retained all stabilizing interactions as found in PM3 most stable and alternative stable conformations of hydroxywybutine (Fig. 1B–F and Table 1).

Interaction between O(6) of tricyclic guanosine ring and hydroxyl group HO(16) of hydroxywybutine side chain of PM3 preferred conformation (Fig. 1B) would be useful to minimize fluctuations that occurred in the $\alpha$ torsion angle of wybutine side chain [21]. Such fluctuations could be important in the frameshifting process as observed in the earlier studies [16–18]. In case of wybutine side chain periodic fluctuations were seen during 2 ns MD simulation study [21]. Hence, presence of OH group in hydroxywybutine side chain might provide extra stability to the hydroxywybutine side chain. Thus, interaction between O(6)···HO(16) might prevent multiple iso-energetic conformations in hydroxywybutine side chain as observed in the wybutine isolated base [21]. This interaction could be helpful to minimize regular fluctuations occurred in $\alpha$ torsion angle during 2 ns of simulation study performed on wybutine molecule [21].

### 4.4. Fluctuations in torsion angles of OHyW during MD

Hydroxywybutine side chain torsion angles and intramolecular hydrogen bonding interactions maintained during 5 ns molecular dynamics simulation performed over the PM3 most stable structure (Fig. 1B) and results are shown in Fig. 4. Torsion angle $\alpha$ was

**Table 3**
Optimized torsion angles of hydroxywybutine after geometry optimizations by RM1, MMFF, HF-SCF and DFT methods.

| Methods | Torsion angles (°) | | | | | | | | | | | Starting geometry |
|---|---|---|---|---|---|---|---|---|---|---|---|---|
| | $\alpha$ | $\beta$ | $\gamma$ | $\eta$ | $\delta$ | $\psi1$ | $\psi2$ | $\theta$ | $\varphi1$ | $\varphi2$ | $\omega$ | |
| RM1 | 272 | 169 | 62 | 301 | 125 | 177 | 180 | 164 | 349 | 186 | 179 | |
| MMFF | 265 | 180 | 66 | 304 | 123 | 180 | 182 | 155 | 350 | 180 | 179 | 1B |
| HF-SCF | 264 | 191 | 69 | 301 | 117 | 179 | 181 | 165 | 352 | 181 | 180 | |
| DFT | 266 | 177 | 64 | 317 | 134 | 179 | 181 | 137 | 347 | 183 | 181 | |

maintained ($\alpha = 270°$) (Fig. 3A) up to 1060 ps and then deviates to $\alpha = 90°$ for the rest of 5 ns MD simulation period. This could be because of interactions between O(6)···$H_1$C(15) and O(6)···HO(16) (Fig. 4A and B) maintained up to 1060 ps. After fluctuation of $\alpha$ torsion angle to 90° hydrogen bonding between O(6)···HO(16) is not possible but the conformation is stabilized by new hydrogen bonding interactions such as O(6)···$H_2$C(15) (Fig. 4G) and O(6)···HC(16) (Fig. 4H) of OHyW side chain. The $\beta$ torsion angle (Fig. 3B) prefers ±180° in order to support extended ('distal') orientation of large side chain i.e. away from five membered imidazole moiety of tricyclic guanosine base. Torsion angle $\gamma$ (Fig. 3C) retains PM3 preferred value ($\gamma = 60°$) up to 1270 ps and then fluctuates to ±60° and ±180° for few picoseconds and finally adopts initial value. Torsion angle $\eta$ (Fig. 3D) maintain its starting geometry with small fluctuations at ±60° and ±180°. These fluctuations could be possible due to interaction between HO(16) with O(6) of tricyclic base and O(23) of hydroxywybutine side chain. Regular fluctuations occurred in $\delta$ torsion angle (Fig. 3E) at ±90° due to presence of weak interactions between O(23)···HC(15) (Fig. 4E) and O(22)···HC(16) (Fig. 4F). Preferred value of $\theta$ (Fig. 3F) and $\varphi1$ (Fig. 3G) torsion angles are maintained throughout simulation study due to presence of O(20)···HC(17) interaction (Fig. 4C). Other torsion angles such as $\psi1$, $\psi2$, $\varphi2$ (Fig. 3H) and $\omega$ maintain starting values throughout the 5 ns simulation period.

All these analyzed torsion angles (Fig. 3) and hydrogen bonding interactions (Fig. 4) during the whole 5 ns simulation period, average (Fig. 2A, B, and F) and snapshot structures (Fig. 2C, D, and E) support the PM3 preferred (Fig. 1B) and alternative conformations (Fig. 1C–F) of hydroxywybutine (OHyW) side chain.

### 4.5. Comparison with isolated wybutine (yW) base

The preferred torsion angles of hydroxywybutine (OHyW) may be compared with isolated wybutine (yW) molecule $\alpha = 90°$, $\beta = 180°$, $\gamma = 300°$, $\delta = 90°$, $\psi1 = 180°$, $\psi2 = 180°$, ±300°, $\theta = 150°$, $\varphi1 = 0°$, $\varphi2 = 180°$ and $\omega = 180°$, ±300° [21]. Torsion angles $\alpha$ and $\gamma$ differs to some extent whereas other torsion angles remains same as compared to wybutine molecule. The preferred conformation of wybutine stabilized by O(6)···HC(15), O(20)···HC(17), O(22)···HC(16) and O(23)···HC(16) intramolecular hydrogen bonding interactions [21], whereas the preferred conformation of hydroxywybutine (Fig. 1B) in this study has also been stabilized by similar kind of hydrogen bonding interactions such as O(6)···HC(15), O(20)···HC(17) and O(22)···HC(16).

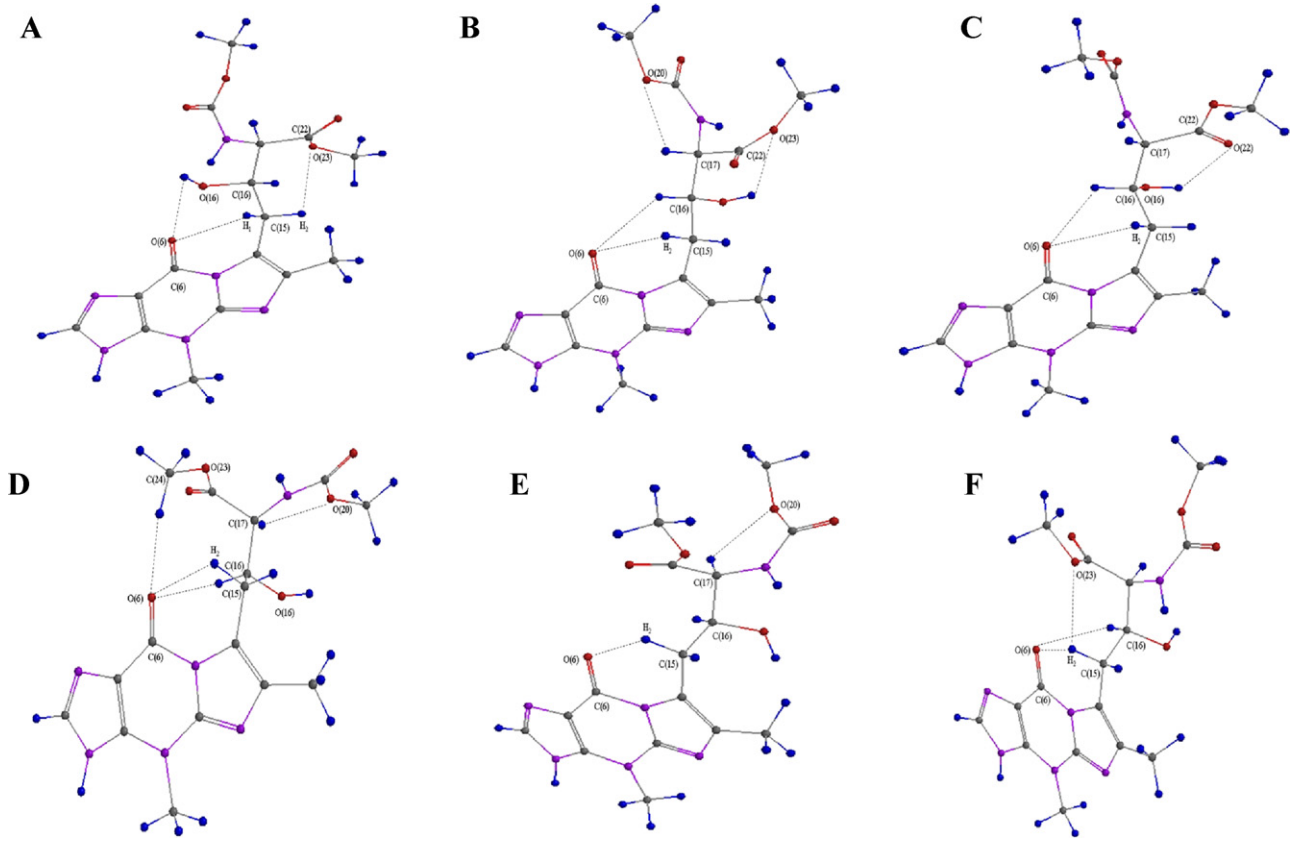


**Fig. 2.** Depicts (A) 0–1000 ps average structure, (B) 2000–2200 ps average structure, (C) 2650 ps snapshot structure, (D) 3590 ps snapshot structure, (E) 4410 ps snapshot structure, and (F) 4900–5000 ps average structure of hydroxywybutine during 5 ns simulation period.

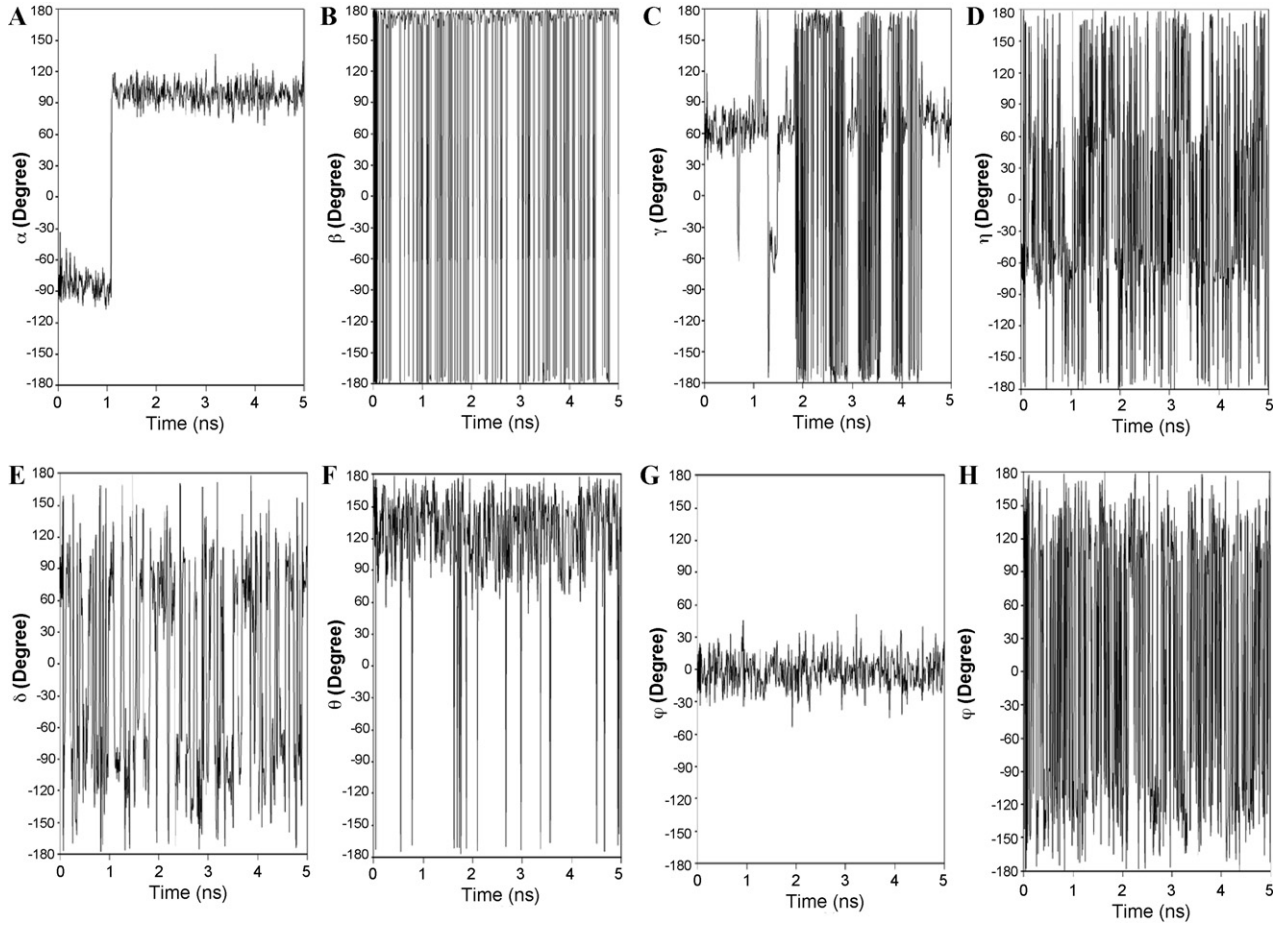


**Fig. 3.** Molecular dynamics (MD) simulation result: (A) showing fluctuation in $\alpha$ torsion angle, (B) fluctuation in $\beta$ torsion angle, (C) fluctuation in $\gamma$ torsion angle, (D) stabilizing values for $\eta$ torsion angle, (E) fluctuation in $\delta$ torsion angle, (F) fluctuation in $\theta$ torsion angle, (G) fluctuation in $\varphi 1$ torsion angle, and (H) stabilizing value for $\varphi 2$ torsion angle.

Additional interactions found in hydroxywybutine side chain are O(6)···HO(16) and O(23)···HC(15). The interaction between O(6)···HO(16) observed because of hydroxyl group present in hydroxywybutine (OHyW) side chain as compared with wybutine (yW) [21]. This O(6)···HO(16) interaction is well maintained in geometry optimized conformations (Table 3) as well as during 5 ns molecular dynamics simulation study up to 1060 ps (Fig. 4B). After words this interaction disrupts till end of the simulation (Fig. 4B). This could be because of fluctuations in the $\alpha$ torsion angle to 90° as shown in Fig. 3A. Regular fluctuations noticed in $\alpha$ and $\delta$ torsion angles of wybutine side chain during 2 ns of simulation study [21] are significantly reduced in case of hydroxywybutine side chain in the present conformational and MD simulation study. Hence, hydrogen bonding interaction between O(6)···HO(16) from the preferred (Fig. 1B) and simulated conformations (Fig. 2A–F) of hydroxywybutine could be able to minimize fluctuations occurred in $\alpha$ torsion angle. It has also noticed that HO(16) also interacts with O(23) of carboxymethyl ($-COOCH_3$) group of OHyW side chain during 5 ns molecular dynamics simulation study. The interaction between O(23)···HO(16) of OHyW side chain might have role to minimize regular fluctuations occurred in $\delta$ torsion angle as compared to wybutine [21]. This carboxymethyl ($-COOCH_3$) group orient towards the $-CH_3$ group of tricyclic ring of guanosine base and might interact with codons if present at 3′-adjacent side of anticodon loop of $tRNA^{Phe}$, similarly as observed in case of wybutine (yW) [21]. Even though hydroxywybutine having different torsion angles as compared to wybutine (yW), it maintains similar type of hydrogen bonding interactions as a stabilizing factor. Hence, the orientation of hydroxywybutine found in this study might help maintain translational reading frame during protein synthesis process by preventing extended Watson–Crick base pairing.

### 4.6. Conformational behavior of hydroxywybutosine in anticodon loop of $tRNA^{Phe}$

Conformational preferences of hydroxywybutosine (OHyW) have also been carried out in the model anticodon loop segment (Me-$C_{m(32)}$-$U_{(33)}$-$G_{m(34)}$-$A_{(35)}$-$A_{(36)}$-$OHyW_{(37)}$-$A_{(38)}$-Me) in presence of 2′-O-methylcytosine (Cm) present at position 32nd and 2′-O-methylguanosine (Gm) at position 34th of yeast $tRNA^{Phe}$. The glycosyl torsion angles ($\chi_{(32)} = 31°$, $\chi_{(33)} = 24°$, $\chi_{(34)} = 3°$, $\chi_{(35)} = 8°$, $\chi_{(36)} = 1°$, $\chi_{(37)} = 22°$, $\chi_{(38)} = 3°$) retained similar values as found in the crystal structure [26]. The set of torsion angles describing PCILO preferred conformation of hydroxywybutosine side chain (Fig. 5B) in the model anticodon loop segment are $\alpha = 120°$, $\beta = 150°$, $\gamma = 300°$, $\eta = 180°$, $\delta = 180°$, $\psi 1 = 180°$, $\psi 2 = 180°$, $\theta = 270°$, $\varphi 1 = 180°$, $\varphi 2 = 180°$ and $\omega = 180°$. The preferred orientation of OHyW in the model anticodon loop segment has been found ‘distal’ i.e. spreads away from the cyclic five membered imidazole moiety of modified tricyclic guanine base similarly as observed in isolated molecule of hydroxywybutine (OHyW) (Figs. 1B–F and 2A–F). The O(19) oxygen from hydroxywybutosine side chain forms inter-residual hydrogen bond with HN(6) of $A_{(36)}$. Preferred conformation of $OHyW_{(37)}$ in anticodon loop segment of yeast $tRNA^{Phe}$ stabilized by O(6)···HC(16), O(22)···HO(16) and O2′···HC(10)

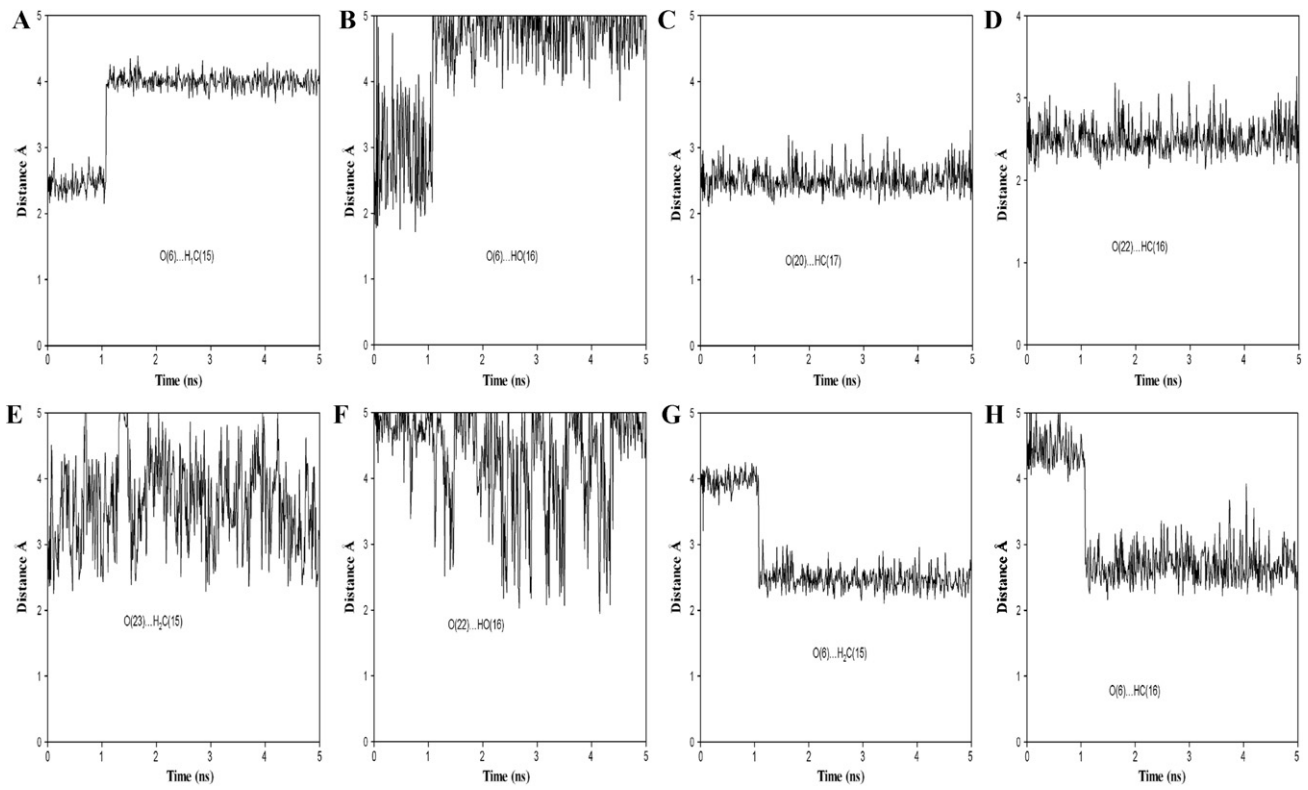


**Fig. 4.** Depicts hydrogen bonding interactions between (A) fluctuation in hydrogen bonding between O(6)···HC(15), (B) O(6)···HO(16), (C) O(20)···HC(17), (D) O(22)···HC(16), (E) O(23)···HC(15), (F) O(22)···HO(16), (G) O(6)···HC(15), and (H) O(6)···HC(16).

**Table 4**
Geometrical analysis of average and snapshot structures of OHyW during 5 ns of MD simulation study.

| Average/snapshot structures (ps) | Torsion angles (°) | Atoms involved (1-2-3) | Distance in pair 1-2 (Å) | Angle 1-2-3 (°) | Fig. ref. |
|---|---|---|---|---|---|
| PM3 most stable structure as starting geometry for molecular dynamics simulation | | | | | |
| 0–1000 | $\alpha = 277^\circ$, $\beta = 178^\circ$, $\gamma = 73^\circ$, $\eta = 277^\circ$, $\delta = 94^\circ$, $\psi 1 = 206^\circ$, $\psi 2 = 237^\circ$, $\theta = 150^\circ$, $\varphi 1 = 357^\circ$, $\varphi 2 = 150^\circ$, $\omega = 181^\circ$. | O(6)···H$_1$C(15) | 2.395 | 111.81 | |
| | | O(6)···HO(16) | 2.116 | 108.67 | 2A |
| | | O(23)···H$_2$C(15) | 2.076 | 141.62 | |
| 1310–1470 | $\alpha = 101^\circ$, $\beta = 178^\circ$, $\gamma = 298^\circ$, $\eta = 103^\circ$, $\delta = 200^\circ$, $\psi 1 = 220^\circ$, $\psi 2 = 136^\circ$, $\theta = 121^\circ$, $\varphi 1 = 352^\circ$, $\varphi 2 = 184^\circ$, $\omega = 174^\circ$. | O(6)···H$_2$C(15) | 2.045 | 113.84 | |
| | | O(6)···HC(16) | 2.038 | 126.01 | 1EHZ.pdb |
| 2000–2200 | $\alpha = 91^\circ$, $\beta = 176^\circ$, $\gamma = 174^\circ$, $\eta = 281^\circ$, $\delta = 104^\circ$, $\psi 1 = 135^\circ$, $\psi 2 = 283^\circ$, $\theta = 126^\circ$, $\varphi 1 = 0^\circ$, $\varphi 2 = 159^\circ$, $\omega = 207^\circ$. | O(6)···H$_2$C(15) | 1.522 | 98.52 | |
| | | O(6)···.HC(16) | 1.757 | 112.44 | 2B |
| | | O(20)···HC(17) | 1.538 | 90.0 | |
| | | O(23)···HO(16) | 2.637 | 94.86 | |
| 2650 | $\alpha = 93^\circ$, $\beta = 176^\circ$, $\gamma = 180^\circ$, $\eta = 303^\circ$, $\delta = 214^\circ$, $\psi 1 = 120^\circ$, $\psi 2 = 150^\circ$, $\theta = 154^\circ$, $\varphi 1 = 359^\circ$, $\varphi 2 = 266^\circ$, $\omega = 119^\circ$. | O(6)···H$_2$C(15) | 2.457 | 110.69 | |
| | | O(6)···.HC(16) | 2.863 | 112.63 | 2C |
| | | O(22)···HO(16) | 2.337 | 126.23 | |
| 3590 | $\alpha = 110^\circ$, $\beta = 178^\circ$, $\gamma = 42^\circ$, $\eta = 313^\circ$, $\delta = 92^\circ$, $\psi 1 = 240^\circ$, $\psi 2 = 221^\circ$, $\theta = 116^\circ$, $\varphi 1 = 346^\circ$, $\varphi 2 = 203^\circ$, $\omega = 150^\circ$. | O(6)···H$_2$C(15) | 2.312 | 112.32 | |
| | | O(6)···.HC(16) | 2.491 | 113.91 | 2D |
| | | O(20)···HC(17) | 2.338 | 92.83 | |
| 4410 | $\alpha = 87^\circ$, $\beta = 178^\circ$, $\gamma = 95^\circ$, $\eta = 6^\circ$, $\delta = 115^\circ$, $\psi 1 = 148^\circ$, $\psi 2 = 187^\circ$, $\theta = 145^\circ$, $\varphi 1 = 348^\circ$, $\varphi 2 = 136^\circ$, $\omega = 180^\circ$. | O(6)···H$_2$C(15) | 2.501 | 105.53 | |
| | | O(6)···.HC(16) | 2.451 | 121.73 | 2E |
| | | O(20)···HC(17) | 2.496 | 94.25 | |
| 4900–5000 | $\alpha = 103^\circ$, $\beta = 174^\circ$, $\gamma = 73^\circ$, $\eta = 161^\circ$, $\delta = 94^\circ$, $\psi 1 = 151^\circ$, $\psi 2 = 110^\circ$, $\theta = 143^\circ$, $\varphi 1 = 5^\circ$, $\varphi 2 = 165^\circ$, $\omega = 232^\circ$. | O(6)···H$_2$C(15) | 2.152 | 108.28 | |
| | | O(6)···.HC(16) | 2.262 | 126.57 | 2F |
| | | O(23)···H$_2$C(15) | 2.391 | 100.80 | |

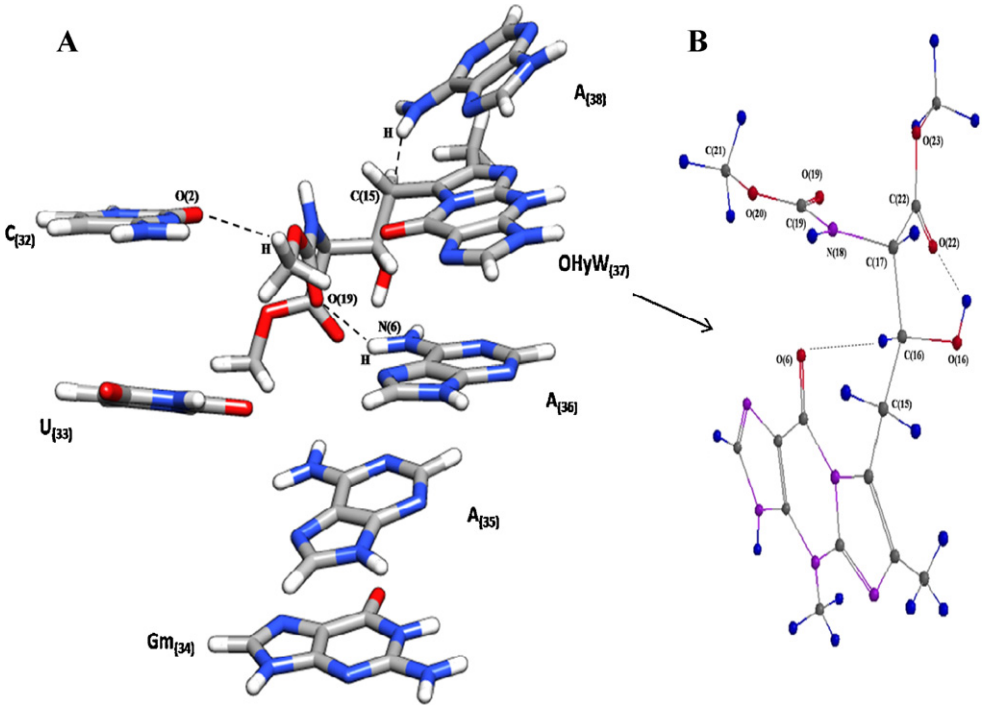


**Fig. 5.** (A) Shows only nucleic acid bases of PCILO preferred stable conformation of anticodon loop of $tRNA^{Phe}$ containing OHyW at 37th position. Anticodon ribose-phosphate backbone are not shown for clarity (B) PCILO preferred stable structure of $OHyW_{(37)}$ extracted from the anticodon loop structure of $tRNA^{Phe}$.

intra-residual as well as O(19)···HN(6)$_{(36)}$, O(2)$_{(32)}$···HC(21)$_{(37)}$ and O2′$_{(33)}$···HN(6)$_{(35)}$ inter-residual hydrogen bonding interactions (Table 5). The hydrogen bonding interaction between O(22)···HO(16) could be responsible to maintain 'distal' conformation of OHyW within the anticodon loop structure of $tRNA^{Phe}$. The preferred orientation of carboxymethyl (—$COOCH_3$) and OH group of hydroxywybutosine side chain i.e. C(22)—O(22)—O(23)—$CH_3$ point towards the —$CH_3$ group of five membered tricyclic ring similarly as found in the isolated molecule of OHyW (Fig. 1B–F) as well as in earlier conformational study of wybutine [21]. Hence, the carboxymethyl (—$COOCH_3$) group of hydroxywybutosine side chain in addition with HO(16) might interact with codons if present at 3′-end and such interactions have been discussed in the earlier work [44,45]. The hydroxywybutosine side chain torsion angles (Fig. 5B) have negligible differences as compared with crystal structure data [26]. Preferred conformation retain interactions between O(6)···HC(16), O2′···HC(10) and O(19)···HN(6)$_{(36)}$ similarly as found in crystal structures (6TNA) of yeast $tRNA^{Phe}$ [26] and 1EHZ [25]. PCILO most stable conformation of $OHyW_{(37)}$ (Fig. 5A and B) preserve similar salient features as found in 1EHZ crystal structure [25]. Torsion angles $\alpha$, $\beta$ and $\gamma$ differs within the range of 0–40° whereas torsion angles $\delta$, $\theta$ and $\varphi 1$ deviated by 71°, 82° and 175°, respectively, as shown in crystal structure [25]. Preferred conformation of $tRNA^{Phe}$ anticodon loop (Fig. 5A) containing OHyW at 37th position significantly preserves hydrogen bonding interactions between O(19) of hydroxywybutosine with HN(6) of 36th base as well as O2′ of 37th ribose ring provides stability by interacting with HC(10) of to tricyclic ring. These interactions were also reported in the crystal structure [25]. Hydrogen bonding between O(19)···HN(6)$_{(36)}$ would be helpful to provide structural stability to $A_{(36)}$ during recognition of UUC codons at the time of protein biosynthesis process.

### 4.7. Geometry optimization of $tRNA^{Phe}$ anticodon loop structure

Salient features of PCILO preferred conformation of hydroxywybutosine present at 37th position in anticodon loop segment of $tRNA^{Phe}$ (Fig. 5A) has been identified by performing automated complete geometry optimization through quantum chemical semi-empirical RM1 and molecular mechanics force field (MMFF) methods. Ribose-phosphate backbone of $tRNA^{Phe}$ anticodon loop segment was freezed whereas only bases were allowed to rotate

**Table 5**
Showing hydrogen bonding interactions from the preferred conformations of OHyW in anticodon loop segment of yeast $tRNA^{Phe}$.

| Atoms involved 1-2-3 | Distance atom pair 1-2 (Å) | Distance atom pair 2-3 (Å) | Angle 1-2-3 (°) | Fig. ref. |
|---|---|---|---|---|
| O(6)···HC(16) | 2.154 | 1.096 | 115.99 | 5 |
| O(22)···HO(16) | 1.984 | 0.958 | 129.43 | 5 |
| O(19)$_{(37)}$···HN(6)$_{(36)}$ | 2.114 | 1.012 | 137.98 | 5 |
| O2′···HC(10) | 2.566 | 1.096 | 135.29 | 5 |
| O2′$_{(33)}$···HN(6)$_{(35)}$ | 1.265 | 1.012 | 137.01 | 5 |
| O5′$_{(33)}$···HC(6)$_{(33)}$ | 1.662 | 1.096 | 167.41 | 5 |
| O5′$_{(32)}$···HC(6)$_{(32)}$ | 2.037 | 1.096 | 159.82 | 5 |
| O5′$_{(35)}$···HC(8)$_{(35)}$ | 2.101 | 1.096 | 154.39 | 5 |
| O(2)$_{(32)}$···HC(21)$_{(37)}$ | 2.469 | 1.096 | 125.09 | 5 |
| O5′$_{(33)}$···HC(6)$_{(33)}$ | 2.161 | 1.096 | 124.83 | 5 |
| O1P$_{(35)}$···HN(3)$_{(32)}$ | 2.380 | 1.012 | 131.72 | 5 |
| N(3)$_{(38)}$···HC3′$_{(38)}$ | 2.494 | 1.096 | 101.61 | 5 |
| N(7)$_{(35)}$···HC(8)$_{(34)}$ | 1.831 | 1.096 | 141.51 | 5 |

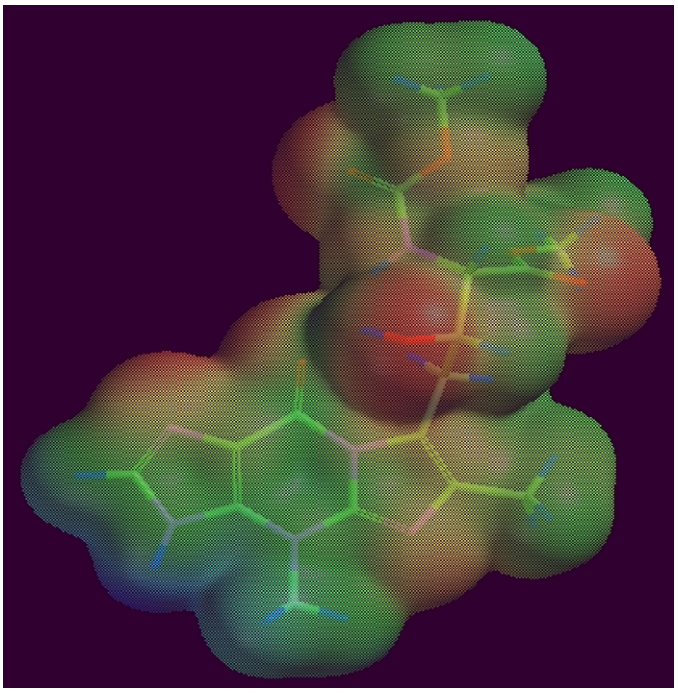

**Fig. 6.** Showing molecular electrostatic potentials (MEPs) calculated for the PM3 preferred most stable structure (Fig. 1B) of isolated hydroxywybutine (OHyW).

freely during the optimization process. RM1 optimized torsion angles of hydroxywybutosine side chain in the model anticodon loop segment of yeast $tRNA^{Phe}$ are ($\alpha = 100^\circ$, $\beta = 173^\circ$, $\gamma = 302^\circ$, $\eta = 138^\circ$, $\delta = 181^\circ$, $\psi 1 = 183^\circ$, $\psi 2 = 178^\circ$, $\theta = 293^\circ$, $\varphi 1 = 173^\circ$, $\varphi 2 = 191^\circ$, $\omega = 179^\circ$). RM1 optimization over PCILO preferred conformation (Fig. 5) show small changes (5–20°) in $\alpha$, $\beta$, $\gamma$, $\delta$, $\psi 1$, $\psi 2$, $\varphi 1$ and $\varphi 2$ torsion angles while torsion angles $\eta$ and $\theta$ differs by 42° and 23°, respectively, from the respective preferred values (Table 5). RM1 optimized structure preserve overall interactions as found in the preferred conformation of hydoxywybutine (Fig. 5B), whereas minor change found in $\alpha$ torsion angle supported by presence of O(6)···HC(15) interaction (Table 1).

The results of MMFF optimization are $\alpha = 77^\circ$, $\beta = 164^\circ$, $\gamma = 312^\circ$, $\eta = 172^\circ$, $\delta = 146^\circ$, $\psi 1 = 184^\circ$, $\psi 2 = 175^\circ$, $\theta = 299^\circ$, $\varphi 1 = 171^\circ$, $\varphi 2 = 184^\circ$, $\omega = 190^\circ$) and may be compared with most stable structure of hydroxywybutosine (Fig. 5B) in anticodon loop segment of yeast $tRNA^{Phe}$. Torsion angles and hydrogen bonding interactions are found in comparison with (Fig. 5B).

### 4.8. Molecular electrostatic potentials (MEPs) and solvent accessible surface area (SASA) calculations

The MEPs for the PM3 most stable structure (Fig. 1B) of hydroxywybutine are calculated and depicted in Fig. 6. The molecular electrostatic potential map of hydroxywybutine shows negative potential for the oxygen atom (red color) which clearly proves that it might serve as hydrogen bond acceptor, while the positive potential (blue color) associated with the hydrogen attached to such a center suggest its role in hydrogen bond donor. Similarly, the intermediate values of the potential are shown in orange, yellow, and green colors (Fig. 6). The atoms O(6), O(16), O(19), O(20), O(22) and O(23) are showing negative potential whereas atom HN(9) shows only positive potential (blue color). The H atom of O(16) indicated by green color showing intermediate values of potentials.

Fig. 7A depicts the solvent accessible surface area (SASA) calculated for PM3 most stable structure obtained for isolated hydroxywybutine (Fig. 1B). Similarly, for the anticodon loop structure of $tRNA^{Phe}$ (Fig. 5) using Chimera software [35] and shown in Fig. 7B and C. The SASA of anticodon loop structure of $tRNA^{Phe}$

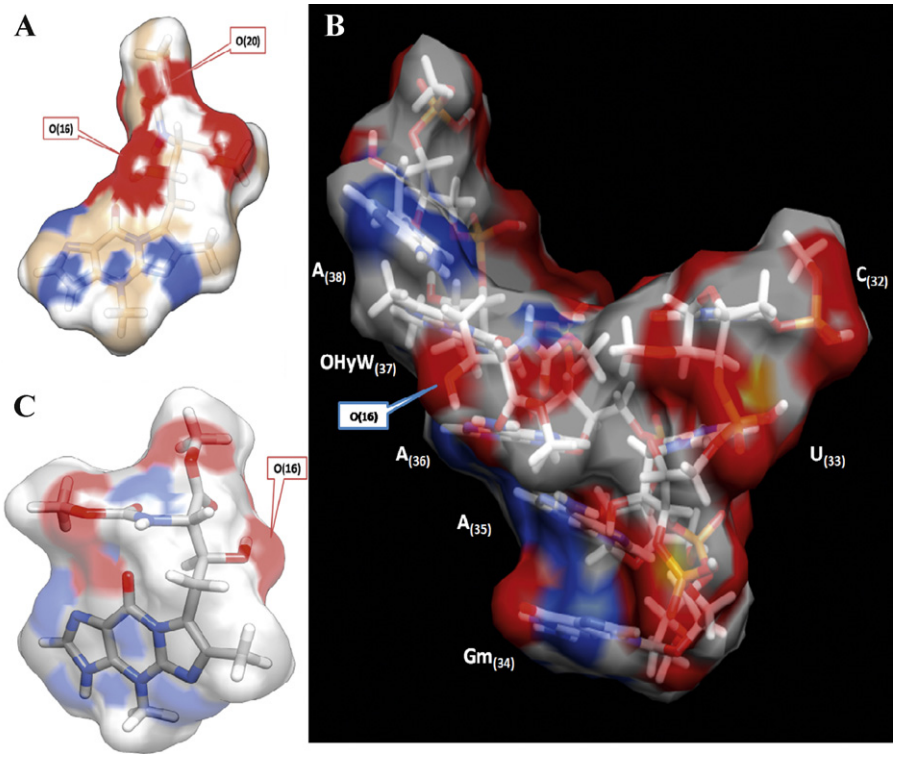


**Fig. 7.** (A) The solvent accessible surface area (SASA) for the PM3 preferred most stable structure (Fig. 1B) of hydroxywybutine (OHyW). (B) SASA of the PCILO preferred stable structure of whole anticodon loop of $tRNA^{Phe}$. (C) SASA calculated for the hydroxywybutosine side chain extracted from the $tRNA^{Phe}$ anticodon loop.

is colored by blue, red and white color. The blue color indicates positively charged atoms such as 'N', red color region indicates negatively charged atoms such as 'O', whereas the white color region shows neutral condition (Fig. 7B). The atoms O(16) of $OHyW_{(37)}$ and O(6) of $Gm_{(34)}$ showing accessibility to solvent (red color) in the anticodon loop structure of $tRNA^{Phe}$ (Fig. 7B). The orientation of HO(16) found in conformational study of $tRNA^{Phe}$ anticodon loop (Figs. 5B and 7C) has also been observed in some alternative higher energy conformations of hydroxywybutine (Fig. 1D–F) as well as in MD simulation study (Fig. 2B–F). Hence, the hydroxyl group, HO(16) of $OHyW_{(37)}$ could play an important role during codon–anticodon interactions.

## 5. Conclusions

The preferred conformation of isolated hydroxywybutine (Fig. 1B) maintain 'distal' orientation and stabilized by hydrogen bonding interactions between O(6)···HC(15), O(6)···HO(16), O(20)···HC(17), O(23)···HC(15), O(22)···HC(16). All these interactions are retained during full geometry optimizations as well during molecular dynamics (MD) simulation study. MD average (Fig. 2A, B, and F) and snapshot (Fig. 2C–E) structures also retained 'distal' conformation of hydroxywybutine side chain as observed in the PM3 most stable conformation (Fig. 1B). The HO(16) group of hydroxywybutine side chain forms hydrogen bond with either O(6) of tricyclic base or O(23) of carboxylic (—$COOCH_3$) group. These interactions O(6)···HO(16) and O(23)···HO(16) could help minimize fluctuations of $\alpha$ and $\delta$ torsion angles that occurred in wybutine molecule [21]. PM3 preferred conformation (Fig. 1B) and MD simulated structures (Fig. 2A–F) of OHyW also preserves orientation of carboxy methyl (—$COOCH_3$) group i.e. C(22)—O(22)—O(23)—$CH_3$ towards the —$CH_3$ group of five membered tricyclic ring. This orientation of carboxy methyl (—$COOCH_3$) group of hydroxywybutine (OHyW) side chain could allow certain kind of interactions with codons if present at 3′-end and such interactions have also been discussed in previous studies [21,44,45].

The molecular electrostatic potentials (MEPs) and solvent accessible surface area (SASA) calculations show that the orientation of HO(16) would be important to interact with either O(6) or O(23) of hydroxywybutine. The interaction between O(19) of hydroxywybutosine with HN(6) of $A_{(36)}$ nucleotide of tRNA anticodon could be helpful to provide structural stability during UUC codon recognition.

Hence, the hypermodified nucleoside hydroxywybutine (OHyW) present at anticodon 3′-adjacent (37th) position of $tRNA^{Phe}$ may prevent extended Watson–Crick base pairing and avoid misreading of genetic information. The hydroxyl (OH) group of hydroxywybutine side chain might be helpful to prevent multiple iso-energetic conformations as observed in the wybutine side chain [21,46]. Thus, hydroxywybutine side chain could play an important role to avoid frameshift mutations. Considering the role of hypermodified nucleosides wybutine (yW) and its derivative hydroxywybutine (OHyW) in the diseases like cancer and HIV [47,48], this study could pave the way to find out molecular reasons behind such deadly diseases.

## Acknowledgements

K. Sonawane is gratefully acknowledged to University Grants Commission, New Delhi for financial support under the major research project. B. Kumbhar expressed his thanks to UGC, New Delhi for fellowship under the UGC SAP DRS-I programme. N. Kumbhar is gratefully acknowledged to Lady Tata Memorial Trust, Mumbai, India, for providing Junior Scholarship.

## References

[1] M. Sprinzl, C. Steegborn, F. Hubel, S. Steinberg, Compilation of tRNA sequences and sequences of tRNA genes, Nucleic Acids Research 24 (1996) 68–72.
[2] P.A. Limbach, P.F. Crain, J.A. McCloskey, Summary the modified nucleosides of RNA, Nucleic Acids Research 22 (1994) 2183–2196.
[3] Y. Motorin, H. Grosjean, Encyclopedia of Life Sciences, Wiley, NY, 2001, pp. 1–9.
[4] T. Suzuki, Biosynthesis and function of tRNA wobble modifications, in: H. Grosjean (Ed.), Fine-tuning of RNA Functions by Modification and Editing, Springer Publisher, NY, 2005, pp. 24–69.
[5] S.H. Blobstein, D. Grunberger, I.B. Weinstein, K. Nakanishi, Isolation and structure determination of the fluorescent base from bovine liver phenylalanine transfer ribonucleic acid, Biochemistry 12 (1973) 188–193.
[6] M. Sprinzl, D.H. Gauss, Compilation of tRNA sequences, Nucleic Acids Research 10 (1982) 1–155.
[7] H. Kasai, Z. Yamaizumi, Y. Kuchino, S. Nishimura, Isolation of hydroxy-Y base from rat liver $tRNA^{Phe}$, Nucleic Acids Research 6 (1979) 993–999.
[8] Y. Kuchino, H. Kasai, Z. Yamaizumi, S. Nishimura, E. Borek, Under modified Y base in a $tRNA^{Phe}$ isoacceptor observed in tumor cells, Biochimica Et Biophysica Acta 565 (1979) 215–218.
[9] Y. Kuchino, E. Borek, D. Grunberger, J.F. Mushinski, S. Nishimura, Change of post-transcriptional modification of wye base in tumor-specific $tRNA^{Phe}$, Nucleic Acids Research 10 (1982) 6421–6432.
[10] R.G. Pergolizzi, D.L. Engelhardt, D. Grunberger, Formation of phenylalanine transfer RNA lacking the Wye base in vero cells during methionine starvation, Journal of Biological Chemistry 253 (1978) 6341–6343.
[11] R.G. Pergolizzi, D.L. Engelhardt, D. Grunberger, Synthesis and coding properties of dinucleoside diphosphates containing alkyl pyrimidines which are formed by the action of carcinogens on nucleic acids, Nucleic Acids Research 6 (1979) 2209–2216.
[12] T. Itaya, N. Watanabe, A. Mizutani, Synthesis of optically active forms of hydroxy-Y base, the minor component of rat liver phenylalanine transfer ribonucleic acid, Tetrahedron Letters 27 (1986) 4043–4046.
[13] T. Itaya, N. Watanabe, T. Iida, T. Kanai, A. Mizutani, Synthesis of β hydroxywybutines, the most probable alternatives for the hypermodified base of rat liver phenylalanine transfer ribonucleic acid, Tetrahedron Letters 51 (1995) 6419–6430.
[14] L.M. Iyer, S. Abhiman, R.F. De Souza, L. Arvind, Origin and evolution of peptide-modifying dioxygenases and identification of the wybutosine hydroxylase/hydroperoxidase, Nucleic Acids Research 38 (2010) 5261–5279.
[15] M. Kato, Y. Araiso, A. Noma, A. Nagao, T. Suzuki, R. Ishitani, O. Nureki, Crystal structure of a novel JmjC-domain-containing protein, TYW5, involved in tRNA modification, Nucleic Acids Research 39 (2011) 1576–1585.
[16] J.N. Li, B. Esberg, J.F. Curran, G.R. Bjork, Three modified nucleosides present in the anticodon stem and loop influence the in vivo aa-tRNA selection in a tRNA-dependent manner, Journal of Molecular Biology 271 (1997) 209–221.
[17] J. Urbonavicius, Q. Qian, J.M. Durand, T.G. Hagervall, G.R. Bjork, Improvement of reading frame maintenance is a common function for several tRNA modifications, EMBO Journal 20 (2001) 4863–4873.
[18] C. Yarian, H. Townsend, W. Czestkowski, E. Sochacka, A.J. Malkiewicz, R. Guenther, A. Miskiewicz, P.F. Agris, Accurate translation of the genetic code depends on tRNA modified nucleosides, Journal of Biological Chemistry 277 (2002) 16391–16395.
[19] P.F. Agris, F.A. Vendeix, W.D. Graham, tRNA's wobble decoding of the genome: 40 years of modification, Journal of Molecular Biology 366 (2007), 1-1.
[20] A. Czerwoniec, S. Dunin-Horkawicz, E. Purta, K.H. Kaminska, J.M. Kasprzak, J.M. Bujnicki, H. Grosjean, K. Rother, MODOMICS: a database of RNA modification pathways. 2008 update, Nucleic Acids Research 37 (2009) D118–D121.
[21] N.M. Kumbhar, K.D. Sonawane, Iso-energetic multiple conformations of hypermodified nucleic acid base wybutine (yW) which occur at 37th position in anticodon loop of $tRNA^{Phe}$, Journal of Molecular Graphics & Modelling 29 (2011) 935–946.
[22] R. Ustabas, N. Suleymanoglu, H. Tanak, Y.B. Alpaslan, Y. Unver, K. Sancak, Experimental and theoretical studies of the molecular structure of 4-(3-(1H-imidazol-1-yl)propyl)-5-p-tolyl-2H-1,2,4-triazol-3(4H)-one, Journal of Molecular Structure 984 (2010) 137–145.
[23] S. Milosavljevi, I. Jurani, I. Aljancic, V. Vajs, N. Todorovi, Conformational analysis of three germacranolides by the PM3 semi-empirical method, Journal of the Serbian Chemical Society 68 (2003) 281–289.
[24] E. Gornicka, E.D. Raczynska, FT-IR spectroscopic, AM1 and PM3 computational studies of conformation of natural products: cytosine, Talanta 57 (2002) 609–616.
[25] H. Shi, P.B. Moore, The crystal structure of yeast phenylalanine transfer RNA at 1.93 Å resolution: a classic structure revisited, RNA 6 (2000) 1091–1105.
[26] S.R. Holbrook, J.L. Sussman, R.W. Warrant, S.H. Kim, Crystal structure of yeast phenylalanine transfer RNA. II. Structural features and functional implications, Journal of Molecular Biology 123 (1978) 631–660.
[27] W.J. Hehre, L. Radom, P.V.R. Schleyer, J.A. Pople, Ab Initio Molecular Orbital Theory, Wiley, NY, 1986.
[28] R.S. Bavi, A.D. Kamble, N.M. Kumbhar, B.V. Kumbhar, K.D. Sonawane, Conformational preferences of modified nucleoside N2-methylguanosine ($m^2G$) and its derivative N2, N2-dimethylguanosine ($m^2{}_2G$) occur at 26th position (hinge region) in tRNA, Cell Biochemistry and Biophysics 61 (2011) 507–552.
[29] S.B. Sambhare, N.M. Kumbhar, A.D. Kamble, B.V. Kumbhar, K.D. Sonawane, Molecular modeling study to investigate conformational preferences and base stacking interactions of hypermodified nucleoside lysidine ($k^2C$) incorporated

in the trinucleotide segment of anticodon loop of tRNA, Bionano Frontier 4 (2011) 191–196.
[30] K.D. Sonawane, U.B. Sonavane, R. Tewari, Conformational flipping of the N(6) substituent in diprotonated N6-(N-glycylcarbonyl) adenines: the role of N(6)H in purine ring protonated ureido adenines, International Journal of Quantum Chemistry 78 (2000) 398–405.
[31] K.D. Sonawane, U.B. Sonavane, R. Tewari, Conformational preferences of anticodon 3-adjacent hypermodified nucleic acid base cis-or trans-Zeatin and its 2-methylthio derivative, cis- or trans-ms$^2$Zeatin, Journal of Biomolecular Structure & Dynamics 19 (2002) 637–648.
[32] K.D. Sonawane, R. Tewari, Conformational preferences of hypermodified nucleoside lysidine (k$^2$C) occurring at 'wobble' position in anticodon loop of tRNA$^{Ile}$, Nucleosides Nucleotides & Nucleic Acids 27 (2008) 1158–1174.
[33] U.B. Sonavane, K.D. Sonawane, A. Morin, H. Grosjean, R. Tewari, N(7)-protonation induced conformational flipping in hypermodified nucleic acid bases N6-(N-threonylcarbonyl) adenine and its 2-methylthio- or N(6)-methylderivatives, International Journal of Quantum Chemistry 75 (1999) 223–229.
[34] U.B. Sonavane, K.D. Sonawane, R. Tewari, Conformational preferences of the base substituent in hypermodified nucleotide queuosine 5-monophosphate 'pQ' and protonated variant 'QH+', Journal of Biomolecular Structure & Dynamics 20 (2002) 437–485.
[35] E.F. Pettersen, T.D. Goddard, C.C. Huang, G.S. Couch, D.M. Greenblatt, E.C. Meng, T.E. Ferrin, UCSF Chimera—a visualization system for exploratory research and analysis, Journal of Computational Chemistry 25 (2004) 1605–1612.
[36] B. Pullman, A. Pullman, Molecular orbital calculations on the conformation of amino acid residues of proteins, Advances in Protein Chemistry 28 (1974) 347–526.
[37] B. Pullman, A. Saran, Quantum-mechanical studies on the conformation of nucleic acid and their constituents, Progress in Nucleic Acid Research and Molecular Biology 18 (1976) 215–325.
[38] G.B. Rocha, R.O. Freire, A.M. Simas, J.J.P. Stewart, RM 1: a reparameterization of AM1 for H, C, N, O, P, S, F, Cl, Br and I, Journal of Computational Chemistry 27 (2006) 1101–1111.
[39] T.A. Halgren, Merck molecular force field. I. Basis, form, scope, parameterization and performance of MMFF94, Journal of Computational Chemistry 17 (1996) 490–519.
[40] A.D. Becke, Density-functional thermochemistry. III. The role of exact exchange, Journal of Chemical Physics 98 (1993) 5648–5652.
[41] M.M. Francl, W.J. Pietro, W.J. Hehre, J.S. Binkley, M.S. Gordon, D.J. Defrees, J.A. Pople, Self-consistent molecular orbital methods. XXIII. A polarization type basis set for second-row elements, Journal of Chemical Physics 77 (1982) 3654–3665.
[42] S. Sharma, U.B. Sonavane, R.R. Joshi, Molecular dynamics simulations of cyclohexyl modified peptide nucleic acids (PNA), Journal of Biomolecular Structure & Dynamics 27 (2010) 663–676.
[43] C.J. Weiner, P.A. Kollman, D.A. Case, U.C. Singh, C. Ghio, G. Alaqom, S. Protera, P.J. Weiner, A new force field for molecular mechanical simulation of nucleic acids and proteins, Journal of the American Chemical Society 106 (1984) 765–784.
[44] M.D. Neto, M.S. Giambiagi, M. Giambiagi, Influence of the hypermodified Y base on the A.U pairing in codon–anticodon interaction, Chemical Physics Letters 290 (1998) 205–210.
[45] A.S. Werneck, M.D. Neto, E.R. Maia, The hypermodified Y base electrostatic contribution to the energetics of the codon–anticodon pairing in tRNA$^{Phe}$, Journal of Molecular Structure-Theochem 427 (1998) 15–23.
[46] F. Claesens, R. Rigler, Conformational dynamics of the anticodon loop in yeast tRNA$^{Phe}$ as sensed by the fluorescence of wybutine, European Biophysics Journal 13 (1986) 331–342.
[47] B.A. Carlson, S.Y. Kwon, M. Chamorro, S. Oroszlan, D.L. Hatfield, B.J. Lee, Transfer RNA modification status influences retroviral ribosomal frameshifting, Virology 255 (1999) 2–8.
[48] D. Hatfield, Y.X. Feng, B.J. Lee, A. Rein, J.G. Levin, S. Roszlan, Chromatographic analysis of the aminoacyl-tRNAs which are required for translation of codons at and around the ribosomal frameshift sites of HIV, HTLV1, and BLV, Virology 173 (1989) 736–742.
[49] I. Majerz, I. Olovsson, Proton-transfer paths in CH···O hydrogen bonds, RSC Advances 2 (2012) 2545–2552.
[50] S. Tsuzuki, T. Uchimaru, M. Mikami, Magnitude of CH/O interactions between carbohydrate and water, Theoretical Chemistry Accounts 131 (2012) 1192–1199.
[51] S. Scheiner, Effect of CH···O hydrogen bond length on the geometric and spectroscopic features of the peptide unit of proteins, International Journal of Quantum Chemistry 110 (2010) 2775–2783.
[52] Q. Li, X. An, B. Gong, J. Cheng, Cooperativity between OH···O and CH···O hydrogen bonds involving dimethyl sulfoxide–$H_2O$–$H_2O$ complex, J. Phys. Chem. A 111 (2007) 10166–10169.
[53] A. Ghosh, M. Bansal, C—H···O hydrogen bonds in minor groove of A-tracts in DNA double helices, Journal of Molecular Biology 294 (1999) 1149–1158.
[54] S. Scheiner, T. Kar, Y. Gu, Strength of the C—H···O hydrogen bond of amino acid residues, Journal of Biological Chemistry 276 (2001) 9832–9837.
[55] M.M. Bhadbhade, R. Kishore, Intramolecular C—H···O hydrogen-bond mediated stabilization of a Cis-$^D$Pro imide-bond in a stereocontrolled heterochiral model peptide, Biopolymers 97 (2011) 73–82.
[56] A.K. Samanta, P. Pandey, B. Bandyopadhyay, T. Chakraborty, Cooperative strengthening of an intramolecular O—H···O hydrogen bond by a weak C—H···O counterpart: matrix-isolation infrared spectroscopy and quantum chemical studies on 3-methyl-1,2-cyclohexanedione, Journal of Physical Chemistry A 114 (2010) 1650–1656.
[57] R. ParthaSarathy, J.M. Ohrt, G.B. Chheda, Modified nucleosides and conformation of anticodon loops: crystal structure of t$^6$A and g$^6$A, Biochemistry 16 (1977) 4999–5008.
[58] A. Parmeggiani, I.M. Krab, T. Watanabe, R.C. Nielsen, C. Dahlberg, J. Nyborg, P. Nissen, Enacyloxin IIa pinpoints a binding pocket of elongation factor Tu for development of novel antibiotics, Journal of Biological Chemistry 281 (2006) 2893–2900.
[59] L. Jiang, L. Lai, CH···O hydrogen bonds at protein–protein interfaces, Journal of Biological Chemistry 277 (2002) 37732–37740.
[60] J. Bella, M. Humphries, Cα—H···O═C hydrogen bonds contribute to the specificity of RGD cell-adhesion interactions, BMC Structural Biology 5 (2005) 4.